Polymer 51 (2010) 1983–1989

Contents lists available at ScienceDirect

Polymer

journal homepage: www.elsevier.com/locate/polymer

Electrospinning and characterization of highly sulfonated polystyrene fibers

Chitrabala Subramanian [a], R.A. Weiss [a,b,c], Montgomery T. Shaw [a,b,*]

[a] Polymer Program, Institute of Materials Science, University of Connecticut, Storrs, CT 06269, USA
[b] Department of Chemical, Materials and Biomolecular Engineering, Chemical Engineering Program, University of Connecticut, Storrs, CT 06269, USA
[c] Department of Polymer Engineering, The University of Akron, Akron, OH 44325, USA

ARTICLE INFO

Article history:
Received 8 December 2009
Received in revised form
22 February 2010
Accepted 28 February 2010
Available online 9 March 2010

Keywords:
Electrospinning
Polyelectrolyte
Sulfonated polystyrene

ABSTRACT

Nanofibers of highly sulfonated (IEC ~4.5 meq/g) polystyrene (SPS) were successfully electrospun. To accomplish this, the process of electrospinning this difficult-to-spin material was studied in detail. Fiber quality was optimized by manipulating the process and solution variables to fabricate continuous bead-free fibers. Bead-free fibers (average diameter 260 nm) were electrospun from 25 wt% SPS (500 kDa) in DMF at an electrode separation of 10 cm, an applied voltage of 16.5 kV and a flow rate of 0.3 mL/h. With increasing solution concentration, and thereby the solution viscosity, the morphology changed from beads to bead-on-string fibers to continuous cylindrical fibers. Beaded fibers and continuous bead-free fibers of SPS (500 kDa) could be spun at ~2 C_e and 3.5 C_e, respectively, where C_e is the entanglement concentration determined from solution-viscosity measurements. The onset of formation of beaded fibers coincided with a sharp transition in the scaling of the storage modulus-concentration relationship.

1. Introduction

Electrospinning has been widely used as a simple technique to fabricate ultra fine fibers from polymer solutions. In contrast to traditional spinning techniques, the driving force for spinning is the electric force generated by the interaction of the applied field with the charges carried by the jet. When a pendant drop of polymer solution is subjected to a high axial voltage gradient, the drop deforms and elongates to form a cone-like structure called a Taylor cone. At a critical voltage a jet is ejected from the cone tip. This jet first traverses a straight path, but this is interrupted by the development of bending instabilities in the jet. At the same time, surface tension exerted by the solution produces a capillary instability that is stabilized by viscoelastic stresses [1]. The jet elongates as a coil due to the electrical forces exerted by the charges carried by the jet. Subsequently, the jet hits the grounded collector, where the charges are neutralized and a solidified nonwoven mat forms [2,3]. Due to their small diameter and high surface area-to-volume ratio, electrospun fibers have been proposed for a wide range of applications, such as filtration, biological scaffolds and sensors.

Although the process of electrospinning neutral polymers is well established, electrospinning of the polyelectrolyte chitosan was reported to be difficult due to the strong repulsive forces between the ionic groups present along the chain [4]. However, other polyelectrolytes have been successfully electrospun into fibers. Examples include sulfonated poly(ether ether ketone) [5,6] poly(2-acrylamido-2-methyl-1-propanesulfonic acid) [7], poly (ethylene-co-vinyl alcohol) sulfonic acid [8], poly(acrylic acid) [9], phospholipids [10] and sulfonated poly(arylene ether sulfone) [11]. The sodium salt of sulfonated polystyrene (Na-SPS) has been electrospun from formic acid and has been used as a base for vapor deposition polymerization to fabricate carbonaceous nanostructures [12].

One application of the latter is as a material for ion-conducting membranes. Sulfonated crosslinked polystyrene (SXLPS) is widely used for ion-exchange applications including proton-exchange membranes (PEMs) for fuel cells [13,14]. Conventional PEM materials, e.g., Nafion®, are random copolymers composed of hydrophobic and acid-containing groups. One limitation of the random-copolymer PEM is that the transport and mechanical properties are coupled, so that optimizing one usually degrades the other. To gain suitable mechanical integrity, the ion-exchange capacities (IEC) of the copolymers are typically held below 2 meq/g, which limits the conductivity of the PEM. As a result, during the past decade there has been a renewed effort to develop new PEM materials, especially composite materials that allow separation of the transport and mechanical properties. To this end, a number of approaches have been considered for designing PEMs, including block copolymers [15], nanofiber-based networks [11] and high-IEC, particle-filled systems [16].

* Corresponding author. Polymer Program, Institute of Materials Science, University of Connecticut, Storrs, CT 06269, USA.
E-mail address: montgomery.shaw@uconn.edu (M.T. Shaw).

0032-3861/$ – see front matter © 2010 Elsevier Ltd. All rights reserved.
doi:10.1016/j.polymer.2010.02.052

The electrical conductivity of any material depends on the concentration of charge carriers and their mobility. Hence, the two most important aspects controlling proton transport in a composite membrane comprising acidic particles dispersed in a non-conducting matrix are the concentration of the acid groups at the particle surface (groups buried within the structure will not exchange easily) and a means for proton transport between the particles. Thus, the desired composite structure is one where the particles form an interconnected structure within the non-conducting matrix. For a given particle volume fraction, particles with higher specific surface area are advantageous because such will trap proportionally fewer sulfonic acid groups within their interior. Similarly, as the particle diameter decreases, the buried acid groups become more accessible when the particles are swollen with water.

One way to guarantee an interconnected structure and increase the specific surface area of the dispersed phase in a composite PEM is to electrospin ionomer or polyelectrolyte nanofibers and embed these in a suitable matrix [11]. Acid-modified nanofiber networks should create proton-exchange pathways within the composite and lead to high conductivity.

Electrospinning of neat Nafion® into fibers has not been successful, although blends with other polymers such as polyethylene oxide, polyvinyl alcohol and poly(acrylic acid) have been electrospun [17–19]. Nafion® solutions consist of primary and secondary aggregate structures due to the hydrophobic interactions of the fluorocarbon backbone and the ionic interactions of the side groups, respectively. These aggregates reduce chain entanglements, and it is believed that the lack of sufficient chain entanglements and the resulting low solution viscosity restricts the spinnability of neat Nafion® [19]. Dimethylformamide (DMF) suppresses the primary aggregate formation in Nafion® solutions by solvation of the fluorocarbon sequences, and the addition of methanol prevents the secondary aggregate formation [19]. These precautions, however, are not sufficient to attain spinnability.

One fix is to add linear polymers, especially amphiphilic polymers, such as poly(acrylic acid), that are soluble in both organic and aqueous solvents and can increase the chain entanglements in solution, leading to improved spinnability [19]. Electrospun Nafion®/polyethylene oxide blend fibers have been used as actuators [20].

SXLPS particles have been used in conjunction with a more flexible matrix material to fabricate composite PEMs [14,21]. Although SPS is water soluble, the polymer in the SXLPS particles does not dissolve or migrate out of the membrane, because the chains are covalently crosslinked. The addition of SXLPS particles can increase the IEC of traditional PEMs and improve their mechanical properties due to low water absorption [14,22] of the particles.

Although SXPLS nanoparticles can be combined with another polymer and spun, SXPLS cannot be electrospun by itself because of its crosslinked nature. However, sulfonated polystyrene (SPS) can first be spun and then crosslinked, or polystyrene (PS) can be spun and then crosslinked and sulfonated. In an approach to the latter route, An et al. [23] fabricated electrospun sulfonated polystyrene mats by treating polystyrene nanofiber mats with 98% sulfuric acid. The maximum IEC achieved was 3.74 meq/g for sulfonation times of about 30 min. For higher sulfonation times, it was expected that there could be structural changes to the electrospun mats, as they were not crosslinked. Hong et al. [24] fabricated electrospun sulfonated polystyrene mats by treating polystyrene mats with chlorosulfonic acid, followed by Pt-metallization to generate porous membranes for ion-exchange application. Alternatively, spinning SPS would lead to high-IEC structures, which could be subsequently stabilized with a hydrophobic matrix or by crosslinking.

This paper describes the electrospinning of nanofibers from solutions of highly sulfonated polystyrene (SPS). The effects of the process and solution variables on fiber diameter and morphology of this polyelectrolyte were studied. The process was optimized to maximize the proportion of bead-free fibers in a non-woven mat. Though the motivation for this research was to use these nanofibers in the construction of composite proton-exchange membranes for fuel cells, these fibers may also be useful in applications such as sensors, filters, ion-exchange media, and catalysts.

2. Experimental

2.1. Materials

The sodium salts of two sulfonated polystyrenes with $M_w = 70{,}000$ g/mol (Na-SPS-70) and 500,000 g/mol (Na-SPS-500) were obtained from Scientific Polymer Products. An ion-exchange resin (Dowex Marathon C, Sigma Aldrich Co.) was used to convert the sodium salt to the sulfonic acid form. N,N-dimethylformamide (DMF) was obtained from Acros Organics (www.acros.com) and was used as received.

2.2. Conversion of SPS (Na form) to SPS (H form)

Since the acid form of sulfonated polystyrene is needed for a PEM application, the two Na-SPS samples were converted to their acid forms (SPS-70 and SPS-500) by passing a 5 wt% solution of the polymer in distilled water through an ion-exchange column. The column consisted of 15 g of Dowex Marathon C packed into a standard burette, ~1.5 cm diameter, to a height of ~9 cm. To remove any residual acid, the resin bed was washed repeatedly using distilled water until the wash water was neutral. A volumetric flow rate of 0.16 mL/s was used, which corresponds to a superficial velocity of 0.85 mm/s. The ion-exchange capacities (IEC) of the SPS products were 4.49 and 4.91 meq/g for SPS-500 and SPS-70, respectively, as determined by titration with 0.01 N NaOH using phenolphthalein. That IEC corresponds to ~81 and 90 sulfonate groups per 100 repeat units for SPS-500 and SPS-70 respectively. The theoretical IEC limit for a fully sulfonated SPS (one sulfonate group per repeat unit) is 5.4 meq/g.

2.3. Electrospinning

The solutions to be spun were prepared by dissolving a weighed amount of the polymer (SPS) in the acid form in either DMF or distilled water under constant stirring at room temperature. A schematic of the electrospinning setup is shown in Fig. 1. A horizontal arrangement was used to prevent dripping of the polymer solution onto the fiber mat. A 1-mL Norm-Ject® syringe was used to extrude the solution, and the tip of the syringe needle (size – 25 G5/8) was connected to the positive terminal of a high-voltage DC source (Gamma High Voltage Research, Inc, ES 30R/DDPM). The flow rate at which the solution was dispensed from the syringe was controlled using a syringe pump (KD Scientific, model number: 780212), and the electrospun fibers were

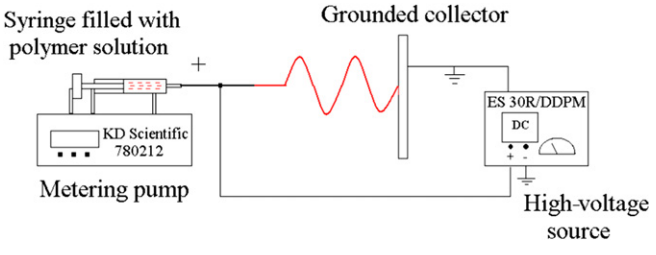

Fig. 1. Schematic of the electrospinning setup.

collected as a non-woven web on a grounded flat metal plate. The spun fibers were stored in a desiccator.

The spinning distance between the needle and collector was varied from 8 to 17 cm in increments of 2 cm. The flow rate at which polymer solution was dispensed from the syringe was varied from 0.1 to 0.7 mL/h in increments of 0.1 mL/h and the applied voltage was varied from 10 to 20 kV. The solution concentration ranged from 10 to 30 wt% of polymer in increments of 5 wt%. Though the relative humidity was not controlled in these experiments, a glove box could be used for the same.

A small section of the product mat was analyzed using a field-emission scanning electron microscope (JEOL JSM-6335F) to determine the product size and morphology. Three different types of products were observed: (1) polymer beads only, (2) bead-on-string, (3) fibers only. The procedure for quantification of the proportion of beads in the product was determined using a modification of the method proposed by Kattamuri and Sung [25] for analyzing electrospun polycarbonate samples. Random sections of high-contrast images were analyzed using Image J software [26] and the number of beads/cm^2 in the electrospun mat was recorded. The areal mass density of the electrospun mat (g/cm^2) was measured by weighing $\sim$1 cm $\times$ 1 cm sections of electrospun fiber mat, and the number of beads per nanogram of mat was calculated.

Table 1 lists the solution and process variables used for electrospinning the two SPS samples in DMF and the morphology of the electrospun mat produced.

2.4. Solution properties

The viscosities of the polymer solutions were measured with a TA Instruments AR-G2, controlled-stress rheometer using a Couette geometry, concentric-cylinder fixture and a stress range of 0.1–100 Pa. The sample temperature was maintained at 25 °C, and the cup was covered to minimize solvent evaporation. The dynamic elastic modulus G' of the solutions was measured using the AR-G2 in the oscillatory mode with a stress amplitude of 0.2 Pa and 10 Pa for SPS-500 and SPS-70 respectively and a frequency range from 0.01 to 100 Hz.

The solution surface tension was measured using a dynamic contact angle analyzer (Cahn DCA-322). A glass microscope cover slip was flame-cleaned prior to use. The DCA analyzer uses the Wilhelmy plate technique in which the glass slip is held perpendicular to the contacting liquid surface. The force changes that occur when the solid surface contacts the liquid are measured by a sensitive balance. The surface tension of the solution is obtained from the equilibrated force on the plate when it is partly immersed in the liquid.

3. Results and discussion

3.1. Effect of solution properties

The bulk solution properties are very important for the electrospinning process [27]. Deitzel et al. [28] have reported that when electrospinning aqueous polyethylene oxide solutions with viscosities lower than 0.1 Pa s, the surface tension controlled the fiber morphology, and beads instead of fibers were favored. For viscosities greater than 2 Pa s, spinning was unachievable due to high viscosities of the polymer solution. At concentrations corresponding to viscosities between 0.1 and 2 Pa s, the electrospun fiber mat was composed of irregular fibers with junctions and bundles at the lower concentrations and uniform cylindrical fibers at the higher concentrations. The surface tensions of the polyethylene oxide solutions were in the range of 35–55 mN/m.

We attempted electrospinning sulfonated polystyrene (SPS) using two different solvents at various solution concentrations. With pure water, the jet had a tendency to break up into droplets, i.e., it electrosprayed rather than electrospin. This can be attributed to the high surface tension of the solvent. DMF worked much better in terms of producing continuous fibers with lower concentration of beads over a wide experimental range. Hence, DMF was used as the solvent for spinning for further analysis.

The molecular weight of the polymer was also an important factor for spinning. With the low-molecular weight polymer, SPS-70, the jet broke up into droplets and produced only beads, see Table 1. It appears that the molecular weight of the polymer was

Table 1
Solution and process variables for electrospinning of SPS-500 in DMF and morphology of the electrospun mat.

SPS molecular weight, kDa	Polymer conc., wt%	Flow rate, mL/h	Solution viscosity, Pa s	Surface tension, N/m	Voltage, kV	Morphology*
70	15	0.2	0.011	0.035	15	B
70	15	0.2	0.011	0.035	18	B
70	15	0.2	0.011	0.035	20	B
70	15	0.2	0.011	0.035	21	B
70	25	0.2	0.083	0.034	15	B
70	25	0.2	0.083	0.034	18	B
70	25	0.2	0.083	0.034	20	B
70	25	0.2	0.083	0.034	25	B
500	10	0.1	0.063	0.036	12	B
500	10	0.1	0.063	0.036	15	B
500	10	0.1	0.063	0.036	18	B
500	10	0.1	0.063	0.036	19	B
500	15	0.1	0.21	0.037	12	B + F
500	15	0.1	0.21	0.037	15	B + F
500	15	0.1	0.21	0.037	18	B + F
500	15	0.1	0.21	0.037	19	B + F
500	20	0.1	0.77	0.04	12	B + F
500	20	0.1	0.77	0.04	15	B + F
500	20	0.1	0.77	0.04	18	B + F
500	20	0.1	0.77	0.04	19	B + F
500	25	0.1	2.99	0.04	12	F
500	25	0.1	2.99	0.04	15	F
500	25	0.1	2.99	0.04	16.5	F
500	25	0.1	2.99	0.04	18	F
500	25	0.1	2.99	0.04	19	F

*B – beads; F – fibers.

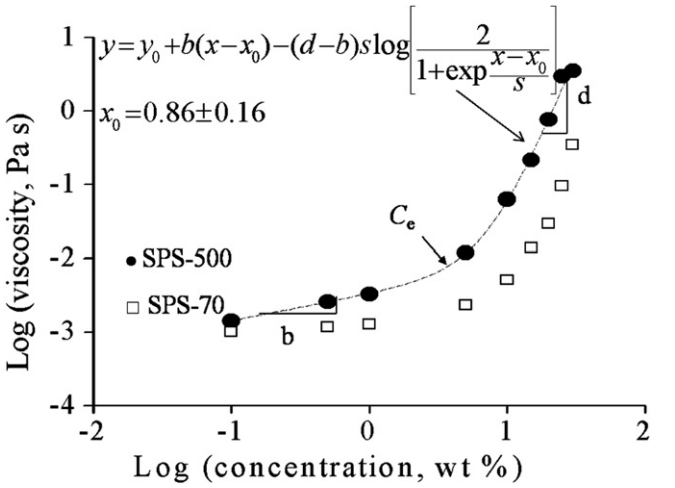

Fig. 2. Viscosity of SPS-500/DMF solutions vs. concentration. With the equation shown, the coefficients, *b* and *d*, correspond to the slope of the curve in the dilute unentangled and entangled chain regimes (see text).

too low for the chains to entangle sufficiently to provide stability to the spinning jet, even at high concentrations. As a consequence of that result, the higher molecular weight polymer, SPS-500, was used for most of the studies. The solutions were spun at room temperature, and the measured relative humidity was in the range of 20–30%.

The solution viscosity of SPS-500 and SPS-70 in DMF are plotted in Fig. 2 as a function of the solution concentration at a constant shear stress of 0.1 Pa. The viscosity increased with concentration, and the variation in viscosity with concentration for SPS-500 was described well by a continuous curve connecting two linear regions. The limiting slopes for the linear regions were obtained by fitting the data to the *continuous kink equation* [29]. A relatively sudden change from a slope $b = 0.36 \pm 0.15$ to a final slope $d = 4.57 \pm 1.13$ occurred at about 7 wt% concentration. The data for the SPS-70 were not described well by this equation, as there are no linear regions over the experimentally measurable range.

For polymer solutions, the entanglement concentration (C_e) corresponds to a transition between dilute, unentangled and entangled chains. At C_e, the polymer chains begin to overlap to form topologically constrained entanglements. For polyelectolytes, C_D is the beginning of the concentrated regime where the electrostatic interactions are highly screened and the solution properties become similar to those of an uncharged polymer [30,31]. Each repeating unit of polyelectrolytes carries a charge. These charges are balanced by a cloud of counter ions in the solution. Due to the electrostatic repulsions between the anions along the polymer backbone, polyelectrolytes have an extended conformation in solvents of high dielectric constant; hence, their viscoelastic behavior differs significantly from neutral polymers. As a result, the semidilute and dilute regimes are extended to higher concentrations relative to a similar polymer with less ionic character or in a less polar solvent.

In Fig. 2, the exponent for the dilute, unentangled regime is in rough agreement with theoretical prediction of 0.5 for polyelectrolytes, while the upper exponent for the entangled regime is in agreement with theoretical prediction of 4.8 for neutral polymers [31,32]. Table 2 lists the theoretical predictions of dependence of specific viscosity of polymer on solution concentration for neutral polymers and polyelectrolytes.

As the concentration of the polymer in the solution was varied for SPS-500, the fiber morphology changed, as shown in Fig. 3.

Table 2
Dependence of specific viscosity of polymer on solution concentration for neutral polymers and polyelectrolytes.

Regime	Neutral Polymers [32]	Polyelectrolytes [31]
Dilute unentangled	$C^{1.25}$	$C^{0.5}$
Dilute entangled	$C^{4.8}$	$C^{1.5}$
Concentrated	$C^{3.6}$	$C^{3.75}$

At relatively low solution concentration, e.g., 10 wt%, the solution electrosprayed and spherical beads were formed (Fig. 3a) as a consequence of Rayleigh instability in the jet due to high surface tension and low elasticity of the solution [5,27]. For a higher concentration, 15 wt%, a bead-on-string morphology was produced, Fig. 3b. At this concentration, bundles of fibers connecting the beads were prevalent. This can be because the fibers fail to dry before reaching the collector, and the wet fibers would have a tendency to fuse and form bundles [33], as well as undergo the Rayleigh instability.

Solution viscosity, which depends on both concentration and molecular weight, has been considered to be the key property that governs both fiber diameter and morphology [34]. At lower solution viscosities, finer fibers with beads occur and at higher viscosities smoother and thicker fibers with a lower proportion of beads are formed. Bead morphology has also been associated with capillary instability. The hypothesis is that at lower concentrations, the chains are insufficiently entangled to provide the high extensional viscosity and strain-hardening behavior required to resist capillary break up of the threadline, leading to bead or bead-on-string morphology. At higher solution concentrations, the higher viscosity stabilizes the fiber, and reduces bead formation [27].

Correspondingly, for the SPS-500/DMF system, increasing the concentration further reduced the proportion of beads, c.f. Figs. 3 c and d. The bead concentration was ~25 beads/ng of electrospun mat for the 15 wt% solution, compared to ~1 beads/ng of electrospun mat for the 20 wt% solution. Above a solution concentration of 25 wt% (~3.5 C_e), continuous, cylindrical, bead-free fibers were produced. The morphology of the product of electrospinning SPS-500/DMF is shown in Fig. 3d and the diameter distribution of the fibers is shown in Fig. 4. This distribution is described adequately by a normal distribution function with $\mu = 265$ nm, $\sigma = 89$ nm.

The observed variation of fiber morphology with concentration is consistent with other reports on different polymers, including charged polymers [5,10,35]. This strongly indicates that chain entanglements are needed to resist capillary instabilities before fibers are formed by the electrospinning process.

A sensitive indicator of entanglements is the dynamic elastic (storage) modulus G'. Fig. 5 shows the variation of G' for the SPS-500/DMF solutions as a function of solution concentration.

The variation in elastic modulus (G') with concentration was also fitted with the continuous kink equation [29]. A relatively sharp change in slope $b = 1.05 \pm 0.52$ to $d = 9.18 \pm 1.08$ was observed at a concentration of about 15 wt% solution. Solutions with concentrations below 15 wt% produced only beads by electrospinning, and above 15 wt% polymer, the morphology consisted of beads attached to the fibers (Fig. 5). The hypothesis is that, the variation in fiber morphology can be related to the solution elasticity. At lower concentrations with low values of G', the jet succumbs to the Rayleigh instability. At a concentration of ~15 wt %, the chain entanglements were sufficient to maintain some fibers, but not high enough to completely eliminate the beads. At even higher concentrations the solution elasticity is high enough to resist the capillary break up and spin continuous bead-free fibers. When the molecular weight was low (SPS-70), spinning was not successful even when the solution viscosity was in the spinning range. Correspondingly, the values of G' for the SPS-70 solutions

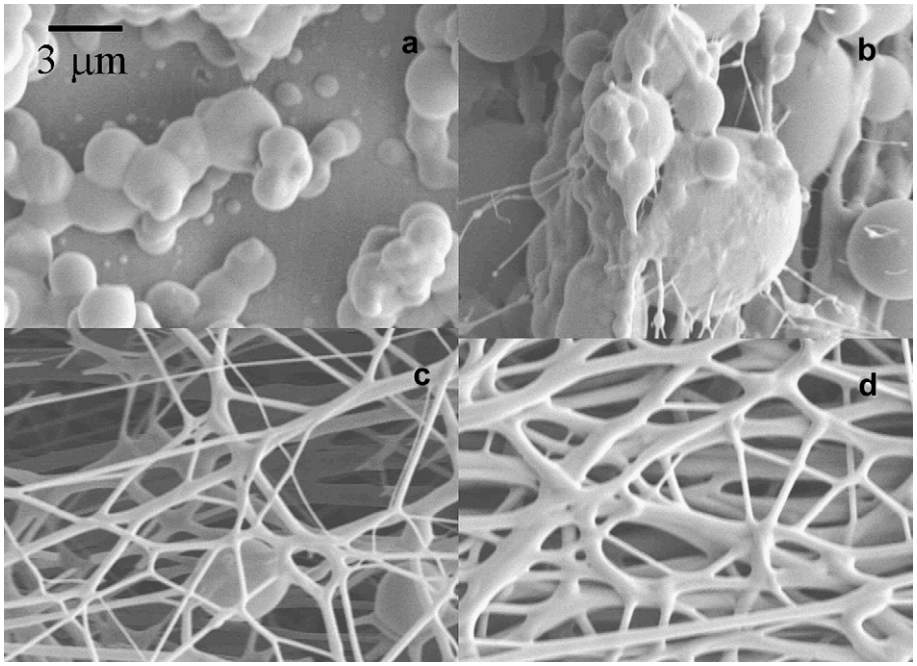

Fig. 3. SEM images of SPS (500 kDa) electrospun at concentrations of (a) 10; (b)15; (c) 20 and (d) 25 wt% in DMF. Field was constant at 0.165 kV/mm.

were too low to be measured, thus demonstrating the importance of entanglements.

The observed role of elasticity is in line with that of other systems such as sodium alginate [36], which was considered difficult to electrospin. However, Nie et al. [36] successfully electrospun sodium alginate by using glycerol as a cosolvent. Rheological measurements indicated an increase in viscosity and elasticity of the system on addition of glycerol. Their explanation was that glycerol, being a polar solvent, would tend to interact with sodium alginate and thus increase flexibility of the chains allowing the chains to entangle. Another example is that provided by Yu et al. [37], who observed that the fluid relaxation time characterizing the solution elasticity was an important factor governing the fiber morphology for polyethylene oxide/polyethylene glycol solutions.

There are other examples of the importance of the entanglement concentration C_e for electrospinning. McKee et al. [38] observed that for linear and branched poly(ethylene terephthalate-*co*-ethylene isophthalate) in 70/30 w/w chloroform/DMF mixture, beaded fibers were formed at C_e and uniform bead-free fibers were formed at ~2–2.5 C_e, where $C_e = 4.5$ and 10 wt% for the linear and branched copolyester, respectively. Polyelectrolytes like poly(2-(dimethylamino)ethyl methacrylate hydrochloride), in 80/20 w/w water/methanol solvent could not be electrospun below 8 C_e ($C_e = 1$ wt%) concentration [30]. Chen et al. [34] reported that ~2 C_e ($C_e = 4$ wt%) was necessary for electrospinning fibers from 1-[2-(methacryloyloxy) ethyl]-3-butylimidazolium tetrafluoroborate in 3/1 w/w acetonitrile/DMF cosolvent. Thus, concentrations well above C_e are desirable to stabilize the jets and spin fibers in the case of polyelectrolytes [30]. Similarly, Shenoy et al. reported that more numerous chain entanglements and associated longer relaxation times prevalent at higher solution concentrations are responsible for continuous fiber spinning, as opposed to bead formation [39].

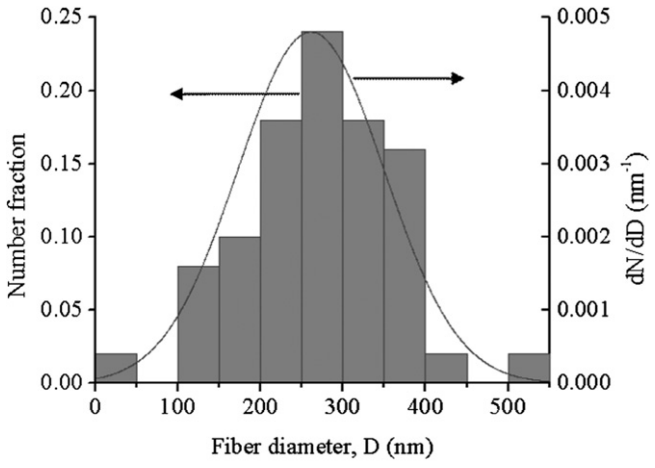

Fig. 4. Fiber diameter distribution for 25 wt% SPS-500 in DMF at 16.5 kV, 10 cm, 0.3 mL/h.

3.2. Effect of process parameters

The variation in fiber diameter of SPS-500 with applied voltage is shown in Fig. 6. The fiber diameters reported represent the mean of measurements from 50 random fibers for each condition. The data in Fig. 6 were fitted using an exponential function. The electrospinning number is defined as $Vq/\gamma R^2$ where V is the voltage, q is the charge (thus Vq is the electrical energy) and γR^2 is the surface free energy [39]. When $Vq/\gamma R^2 > 1$, a jet is ejected from the Taylor cone. As the applied voltage increases, the electrostatic forces acting on the polymer drop also increase, which provides an additional force to overcome the viscoelastic and surface tension forces exerted by the polymer solution. Thus, increasing electrospinning number should increase the elongation of the polymer chains in the jet and produce a finer fiber. This is demonstrated by the data shown in Fig. 6.

Increasing the distance between electrodes had no observable effect on the electrospun SPS-500/DMF fibers over the range where spinning was achieved. At relatively high flow rates, ≥0.4 mL/h, the spinning process was not continuous and intermittent dripping of polymer solution onto the collector was observed. Kattamuri et al. [25] reported that very low and high flow rates are not desirable. At low flow rates maintaining a continuous stream is difficult, while at

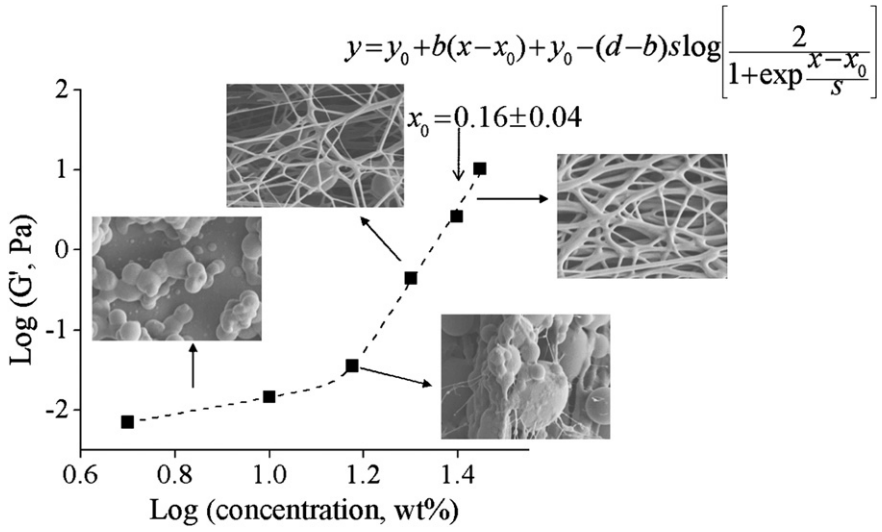

Fig. 5. Plot of G′ vs. solution concentration for SPS-500 solution in DMF at a frequency of 1 Hz.

very high flow rates, the polymer jet shoots out too quickly and hence fibers are not formed.

Though the solution and process variables had a large qualitative effect on the fiber morphology, their influence on the fiber diameter was not very prominent. This is consistent with previous work on electrospinning of polyvinylidene fluoride [27]. The hygroscopic nature of the sulfonated polymer made spinning difficult at higher relative humidity. At a relative humidity of ~35% the fibers piled up onto the collector and the fiber bundle had a tendency to stretch from the collector towards the needle. A similar behavior was observed by Laforgue et al. [18] while electrospinning Nafion-polyethylene oxide and Nafion-polyvinyl alcohol blends and by Okuzaki et al. [40] while electrospinning poly (*p*-xylenetetrahydrothiophenium chloride). Laforgue et al. [18] have explained these observations in terms of the ion-conducting nature of polyelectrolytes in the presence of water in ambient air. Their hypothesis was that, initially few short fibers deposit vertically onto the collector. The solvent in the polymer jet does not evaporate easily due to high humidity of the surrounding air and hence the nanofibers are highly conducting. These conducting nanofibers become the shortest distance to grounded flat plate collector. Additional fibers accumulate onto the initially deposited fibers and eventually grow to form a column of fiber between the two electrodes. At very high relative humidity (>40%) the electrospun SPS-500/DMF fibers fuse and form a film on the collector.

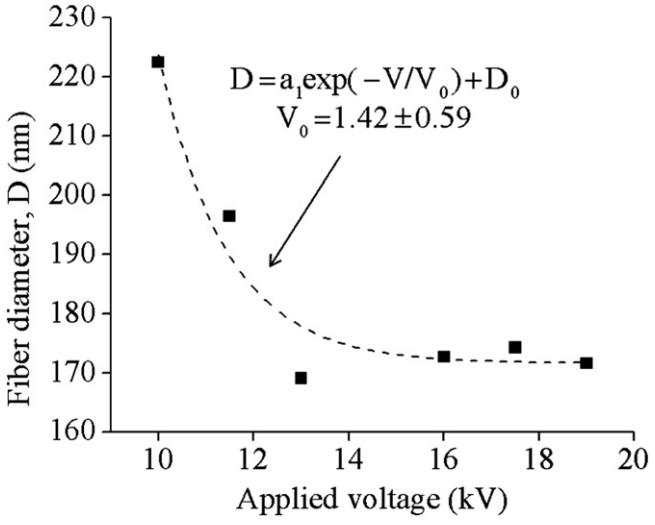

Fig. 6. Effect of applied voltage on electrospinning of 25 wt% SPS in DMF at 0.3 mL/h, 10 cm.

4. Conclusions

Highly sulfonated (IEC = 4.5 meq/g) polystyrene (SPS) nanofibers were successfully produced by electrospinning. In this study, bead-free fibers were electrospun from a 25 wt% polymer solution of 500-kDa SPS in DMF. The process variables were roughly optimal at an applied voltage of 16.5 kV, a 10-cm electrode separation and a flow rate of 0.3 mL/h. The average fiber diameter was 260 nm under these conditions. The morphology of the electrospun product changed, with increasing solution concentration, from beads to bead-on-string fibers to continuous cylindrical fibers. Increasing the solution concentration increased the solution viscosity, which improved the spinnability of continuous fibers. A change in scaling of the viscosity-concentration relationship occurred at a critical concentration, C_e of 7 wt% polymer, where the scaling exponents changed from 0.36 ± 0.15 and 4.57 ± 1.13 at low and high concentrations, respectively. For the 500 kDa SPS in DMF, a polymer concentration of 3.5 C_e (~ 25 wt% polymer) was required for the production of continuous, bead-free fibers.

A sharp change in the storage modulus-concentration scaling was observed at about 15 wt% concentration for 500-kDa SPS solutions. The onset of bead-on-string fiber formation coincided with the transition in the storage modulus-concentration scaling, which most likely is the onset of the formation of entanglements in the polymer solution. Lower molecular weight (70 kDa) SPS solutions could not be spun in spite of having viscosities in the spinning range observed for the 500-kDa solutions. Correspondingly, the values of the storage modulus for the concentrated 70-kDa solutions were low, suggesting that entanglements are not just desirable, but necessary for spinning of SPS/DMF solutions.

Acknowledgements

Financial support was provided by the Civil, Mechanical and Manufacturing Innovation Program (Directorate of Engineering) of the National Science Foundation, Grant CMMI grant #0727545.

References

[1] Theron SA, Zussman E, Yarin AL. Polymer 2004;45(6):2017–30.
[2] Reneker DH, Chun I. Nanotechn 1996;7(3):216–23.

[3] Reneker DH, Yarin AL. Polymer 2008;49(10):2387–425.
[4] Park W, Jeong L, Yoo D, Hudson S. Polymer 2004;45(21):7151–7.
[5] Li X, Hao X, Xu D, Zhang G, Zhong S, Na H, et al. J Membr Sci 2006;281(1–2):1–6.
[6] Li X, Hao X, Na H. Mater Lett 2007;61(2):421–6.
[7] Kim SJ, Lim JY, Kim IY, Lee SH, Lee TS. Smart Mater Struct 2005;14(4):N16–20.
[8] Jin, W. Z., Duan, H. W., Zhang, Y. J., Li, F. F. Presented at the Proceedings of the 1st International conference on nano/micro engineered and macromolecular systems Zhuhai, China, 2006.
[9] Li L, Hsieh YL. Polymer 2005;46(14):5133–9.
[10] McKee MG, Layman JM, Cashion MP, Long TE. Science 2006;311(5759):353–5.
[11] Choi J, Kyun ML, Ryszard W, Pintauro PN, Mather PT. Macromolecules 2008;41(13):4569–72.
[12] McCann JT, Lim B, Ostermann R, Rycenga M, Marquez M, Xia Y. Nano Lett 2007;7(8):2470–4.
[13] Chen SL, Krishnan L, Srinivasan S, Benziger J, Bocarsly AB. J Membr Sci 2004;243(1-2):327–33.
[14] Brijmohan SB, Shaw MT. Polymer 2006;47(8):2856–64.
[15] Ehrenberg SG, Wnek GEU. S. Pat 2002;6383391.
[16] Hong L, Chen N. J Polym Sci 2000;38(11):1530–8.
[17] Sanders EH, McGrady KA, Wnek GE, Edmondson CA, Mueller JM, Fontenella JJ, et al. J Power Sources 2004;129(1):55–61.
[18] Laforgue A, Robitaille L, Mokrini A, Ajji A. Macromol Mater Eng 2007;292(12):1229–36.
[19] Chen H, Snyder JD, Elabd YA. Macromolecules 2008;41(1):128–35.
[20] Nah C, Kwak SK, Kim N, Lyu MY, Hwang BS, Akle B, et al. Key Eng Mater 2007;334-335:1001–4.
[21] Oren Y, Freger V, Linder C. J Membr Sci 2004;239(1):17–26.
[22] Gasa JV, Brijmohan SB, Weiss RA, Shaw MT. J Membr Sci 2006;269(1-2):177–86.
[23] An H, Chase GG. J Membr Sci 2006;283(1-2):84–7.
[24] Hong SH, Lee SA, Nam JD, Lee YK, Kim TS, Won S. Macromol Res 2008;16(3):204–11.
[25] Kattamuri N, Sung C. NSTI-Nanotech 2004;3:425–8.
[26] Available from <http://rsbweb.nih.gov/ij/>.
[27] Chanunpanich N, Lee B, Byun H. Macromol Res 2008;16(3):212–7.
[28] Deitzel JM, Kleinmeyer J, Harris D, Beck Tan NC. Polymer 2001;42(1):261–72.
[29] Shaw MT. J Rheol 2007;51(6):1303–18.
[30] McKee MG, Hunley MT, Layman JM, Long TE. Macromolecules 2006;39(2):575–83.
[31] Rubinstein M, Colby RH, Dobrynin AV. Phys Rev Lett 1994;73(2):2776–9.
[32] de Gennes PG. Scaling concepts in polymer physics. 1st ed. Ithaca and London: Cornell University Press; 1979.
[33] Cui W, Li X, Zhou S, Weng J. J Appl Polym Sci 2007;103(5):3105–12.
[34] Chen H, Elabd YA. Macromolecules 2009;42(9):3368–73.
[35] Heikkila P, Harlin A. Eur Polym J 2008;44(10):3067–79.
[36] Nie H, He A, Zheng J, Xu S, Li J, Han CC. Biomacromolecules 2008;9(5):1362–5.
[37] Yu JH, Fridrikh SV, Rutledge GC. Polymer 2006;47(13):4789–97.
[38] McKee MG, Wilkes GL, Colby RH, Long TE. Macromolecules 2004;37(5):1760–7.
[39] Shenoy SL, Bates WD, Frisch HL, Wnek GE. Polymer 2005;46(10):3372–84.
[40] Okuzaki H, Takahashi T, Miyajima N, Suzuki Y, Kuwabara T. Macromolecules 2006;39(13):4276–8.